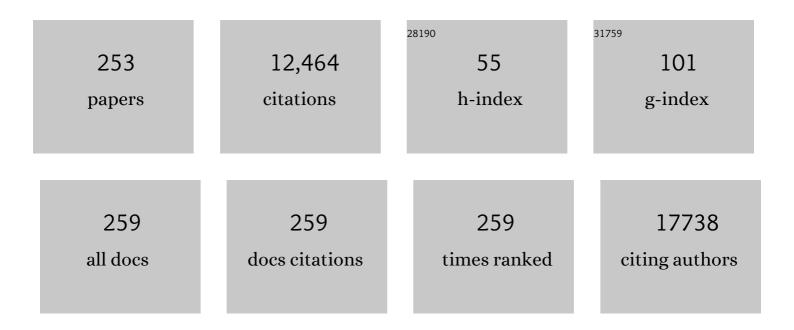
Yizhong Huang

List of Publications by Year in descending order

Source: https://exaly.com/author-pdf/8447253/publications.pdf Version: 2024-02-01



#	Article	IF	CITATIONS
1	Synthesis of hexagonal close-packed gold nanostructures. Nature Communications, 2011, 2, 292.	5.8	553
2	Nickel Nanoparticles Encapsulated in Few‣ayer Nitrogenâ€Ðoped Graphene Derived from Metal–Organic Frameworks as Efficient Bifunctional Electrocatalysts for Overall Water Splitting. Advanced Materials, 2017, 29, 1605957.	11.1	507
3	Zeolitic Imidazolate Framework 67â€Derived High Symmetric Porous Co ₃ O ₄ Hollow Dodecahedra with Highly Enhanced Lithium Storage Capability. Small, 2014, 10, 1932-1938.	5.2	442
4	MOF-templated formation of porous CuO hollow octahedra for lithium-ion battery anode materials. Journal of Materials Chemistry A, 2013, 1, 11126.	5.2	361
5	A Flexible Alkaline Rechargeable Ni/Fe Battery Based on Graphene Foam/Carbon Nanotubes Hybrid Film. Nano Letters, 2014, 14, 7180-7187.	4.5	346
6	Highâ€Performance Asymmetric Supercapacitors Based on Multilayer MnO ₂ /Graphene Oxide Nanoflakes and Hierarchical Porous Carbon with Enhanced Cycling Stability. Small, 2015, 11, 1310-1319.	5.2	326
7	Investigating the Role of Tunable Nitrogen Vacancies in Graphitic Carbon Nitride Nanosheets for Efficient Visible-Light-Driven H ₂ Evolution and CO ₂ Reduction. ACS Sustainable Chemistry and Engineering, 2017, 5, 7260-7268.	3.2	322
8	GaAs/AlGaAs Nanowire Photodetector. Nano Letters, 2014, 14, 2688-2693.	4.5	256
9	Highly Efficient Restoration of Graphitic Structure in Graphene Oxide Using Alcohol Vapors. ACS Nano, 2010, 4, 5285-5292.	7.3	242
10	Investigation of microstructure and mechanical properties of Al6061-nanocomposite fabricated by stir casting. Materials & Design, 2014, 55, 921-928.	5.1	230
11	Interpenetrating interfaces for efficient perovskite solar cells with high operational stability and mechanical robustness. Nature Communications, 2021, 12, 973.	5.8	189
12	FeCo/FeCoNi/N-doped carbon nanotubes grafted polyhedron-derived hybrid fibers as bifunctional oxygen electrocatalysts for durable rechargeable zinc–air battery. Applied Catalysis B: Environmental, 2019, 254, 26-36.	10.8	183
13	Molten-salt-mediated synthesis of SiC nanowires for microwave absorption applications. CrystEngComm, 2013, 15, 570-576.	1.3	182
14	Largeâ€Area and Highâ€Quality 2D Transition Metal Telluride. Advanced Materials, 2017, 29, 1603471.	11.1	181
15	Ultrafine Metal Nanoparticles/Nâ€Doped Porous Carbon Hybrids Coated on Carbon Fibers as Flexible and Binderâ€Free Water Splitting Catalysts. Advanced Energy Materials, 2017, 7, 1700220.	10.2	156
16	Structure stability of metal-organic framework MIL-53 (Al) in aqueous solutions. International Journal of Hydrogen Energy, 2013, 38, 16710-16715.	3.8	153
17	Van der Waals negative capacitance transistors. Nature Communications, 2019, 10, 3037.	5.8	144
18	Novel fuel cell with nanocomposite functional layer designed by perovskite solar cell principle. Nano Energy, 2016, 19, 156-164.	8.2	137

#	Article	IF	CITATIONS
19	Exploring the impact of atomic lattice deformation on oxygen evolution reactions based on a sub-5 nm pure face-centred cubic high-entropy alloy electrocatalyst. Journal of Materials Chemistry A, 2020, 8, 11938-11947.	5.2	137
20	Graphene Oxideâ€Templated Synthesis of Ultrathin or Tadpoleâ€Shaped Au Nanowires with Alternating <i>hcp</i> and <i>fcc</i> Domains. Advanced Materials, 2012, 24, 979-983.	11.1	135
21	General Approach for MOF-Derived Porous Spinel AFe ₂ O ₄ Hollow Structures and Their Superior Lithium Storage Properties. ACS Applied Materials & Interfaces, 2015, 7, 26751-26757.	4.0	133
22	Unraveling the Potassium Storage Mechanism in Graphite Foam. Advanced Energy Materials, 2019, 9, 1900579.	10.2	133
23	Controllable Growth of ZnO Nanostructures by a Simple Solvothermal Process. Journal of Physical Chemistry C, 2008, 112, 106-111.	1.5	132
24	Full Solutionâ€Processed Synthesis of All Metal Oxideâ€Based Treeâ€like Heterostructures on Fluorineâ€Doped Tin Oxide for Water Splitting. Advanced Materials, 2012, 24, 5374-5378.	11.1	131
25	Defective ultra-thin two-dimensional g-C3N4 photocatalyst for enhanced photocatalytic H2 evolution activity. Journal of Colloid and Interface Science, 2021, 581, 159-166.	5.0	125
26	Phase-controllable growth of ultrathin 2D magnetic FeTe crystals. Nature Communications, 2020, 11, 3729.	5.8	120
27	In situ Raman spectroscopy study of corrosion products on the surface of carbon steel in solution containing Clâ [~] and <mml:math altimg="si1.gif" overflow="scroll" xmlns:mml="http://www.w3.org/1998/Math/MathML"><mml:mrow><mml:mtext>SO</mml:mtext></mml:mrow><mml:mrow><mml:mrow><mml:mrow><mml:mtext>SO</mml:mtext></mml:mrow><mml:mrow><mml:mrow><mml:mtext>SO</mml:mtext></mml:mrow><mml:mrow><mml:mrow><mml:mrow><mml:mrow><mml:mrow><mml:mrow><mml:mrow><mml:mrow><mml:mrow><mml:mrow><mml:mrow><mml:mrow><mml:mrow><mml:mrow><mml:mrow><mml:mrow><mml:mrow><mml:mrow><mml:mrow><mml:mrow><mml:mrow><mml:mrow><mml:mrow><mml:mrow><mml:mrow><mml:mrow><mml:mrow><mml:mrow><mml:mrow><mml:mrow><mml:mrow><mml:mrow><mml:mrow><mml:mrow><mml:mrow><mml:mrow><mml:mrow><mml:mrow><mml:mrow><mml:mrow><mml:mrow><mml:mrow><mml:mrow><mml:mrow><mml:mrow><mml:mrow><mml:mrow><mml:mrow><mml:mrow><mml:mrow><mml:mrow><mml:mrow><mml:mrow><mml:mrow><mml:mrow><mml:mrow><mml:mrow><mml:mrow><mml:mrow><mml:mrow><mml:mrow><mml:mrow><mml:mrow><mml:mrow><mml:mrow><mml:mrow><mml:mrow><mml:mrow><mml:mrow><mml:mrow><mml:mrow><mml:mrow><mml:mrow><mml:mrow><mml:mrow><mml:mrow><mml:mrow><mml:mrow><mml:mrow><mml:mrow><mml:mrow><mml:mrow><mml:mrow><mml:mrow><mml:mrow><mml:mrow><mml:mrow><mml:mrow><mml:mrow><mml:mrow><mml:mrow><mml:mrow><mml:mrow><mml:mrow><mml:mrow><mml:mrow><mml:mrow><mml:mrow><mml:mrow><mml:mrow><mml:mrow><mml:mrow><mml:mrow><mml:mrow><mml:mrow><mml:mrow><mml:mrow><mml:mrow><mml:mrow><mml:mrow><mml:mrow><mml:mrow><mml:mrow><mml:mrow><mml:mrow><mml:mrow><mml:mrow><mml:mrow><mml:mrow><mml:mrow><mml:mrow><mml:mrow><mml:mrow><mml:mrow><mml:mrow><mml:mrow><mml:mrow><mml:mrow><mml:mrow><mml:mrow><mml:mrow><mml:mrow><mml:mrow><mml:mrow><mml:mrow><mml:mrow><mml:mrow><mml:mrow><mml:mrow><mml:mrow><mml:mrow><mml:mrow><mml:mrow><mml:mrow><mml:mrow><mml:mrow><mml:mrow><mml:mrow><mml:mrow><mml:mrow><mml:mrow><mml:mrow><mml:mrow><mml:mrow><mml:mrow><mml:mrow><mml:mrow><mml:mrow><mml:mrow><mml:mrow><mml:mrow><mml:mrow><mml:mrow><mml:mrow><mml:mrow><mml:mrow><mml:m< td=""><td>l:mrow><</td><td>mmi:mn>4<</td></mml:m<></mml:mrow></mml:mrow></mml:mrow></mml:mrow></mml:mrow></mml:mrow></mml:mrow></mml:mrow></mml:mrow></mml:mrow></mml:mrow></mml:mrow></mml:mrow></mml:mrow></mml:mrow></mml:mrow></mml:mrow></mml:mrow></mml:mrow></mml:mrow></mml:mrow></mml:mrow></mml:mrow></mml:mrow></mml:mrow></mml:mrow></mml:mrow></mml:mrow></mml:mrow></mml:mrow></mml:mrow></mml:mrow></mml:mrow></mml:mrow></mml:mrow></mml:mrow></mml:mrow></mml:mrow></mml:mrow></mml:mrow></mml:mrow></mml:mrow></mml:mrow></mml:mrow></mml:mrow></mml:mrow></mml:mrow></mml:mrow></mml:mrow></mml:mrow></mml:mrow></mml:mrow></mml:mrow></mml:mrow></mml:mrow></mml:mrow></mml:mrow></mml:mrow></mml:mrow></mml:mrow></mml:mrow></mml:mrow></mml:mrow></mml:mrow></mml:mrow></mml:mrow></mml:mrow></mml:mrow></mml:mrow></mml:mrow></mml:mrow></mml:mrow></mml:mrow></mml:mrow></mml:mrow></mml:mrow></mml:mrow></mml:mrow></mml:mrow></mml:mrow></mml:mrow></mml:mrow></mml:mrow></mml:mrow></mml:mrow></mml:mrow></mml:mrow></mml:mrow></mml:mrow></mml:mrow></mml:mrow></mml:mrow></mml:mrow></mml:mrow></mml:mrow></mml:mrow></mml:mrow></mml:mrow></mml:mrow></mml:mrow></mml:mrow></mml:mrow></mml:mrow></mml:mrow></mml:mrow></mml:mrow></mml:mrow></mml:mrow></mml:mrow></mml:mrow></mml:mrow></mml:mrow></mml:mrow></mml:mrow></mml:mrow></mml:mrow></mml:mrow></mml:mrow></mml:mrow></mml:mrow></mml:mrow></mml:mrow></mml:mrow></mml:mrow></mml:mrow></mml:mrow></mml:mrow></mml:mrow></mml:mrow></mml:mrow></mml:mrow></mml:mrow></mml:mrow></mml:mrow></mml:mrow></mml:mrow></mml:mrow></mml:mrow></mml:mrow></mml:mrow></mml:mrow></mml:mrow></mml:mrow></mml:mrow></mml:mrow></mml:mrow></mml:mrow></mml:mrow></mml:mrow></mml:mrow></mml:mrow></mml:mrow></mml:mrow></mml:mrow></mml:mrow></mml:mrow></mml:mrow></mml:mrow></mml:mrow></mml:mrow></mml:mrow></mml:mrow></mml:mrow></mml:mrow></mml:mrow></mml:mrow></mml:mrow></mml:mrow></mml:mrow></mml:math>	l:mrow><	mmi:mn>4<
28	Human Gait Recognition Using Patch Distribution Feature and Locality-Constrained Group Sparse Representation. IEEE Transactions on Image Processing, 2012, 21, 316-326.	6.0	116
29	Rapid Pseudocapacitive Sodiumâ€lon Response Induced by 2D Ultrathin Tin Monoxide Nanoarrays. Advanced Functional Materials, 2017, 27, 1606232.	7.8	108
30	Polydopamine-assisted decoration of ZnO nanorods with Ag nanoparticles: an improved photoelectrochemical anode. Journal of Materials Chemistry A, 2013, 1, 5045-5052.	5.2	104
31	Synthesis of multimodal porous ZnCo2O4 and its electrochemical properties as an anode material for lithium ion batteries. Journal of Power Sources, 2015, 294, 112-119.	4.0	99
32	Manganese phosphate coated Li[Ni0.6Co0.2Mn0.2]O2 cathode material: Towards superior cycling stability at elevated temperature and high voltage. Journal of Power Sources, 2018, 402, 263-271.	4.0	99
33	Highly dispersed Au nanoparticles immobilized on Zr-based metal–organic frameworks as heterostructured catalyst for CO oxidation. Journal of Materials Chemistry A, 2013, 1, 14294.	5.2	95
34	Transitionâ€Metalâ€Ionâ€Mediated Polymerization of Dopamine: Musselâ€Inspired Approach for the Facile Synthesis of Robust Transitionâ€Metal Nanoparticle–Graphene Hybrids. Chemistry - A European Journal, 2014, 20, 7776-7783.	1.7	95
35	"Electron/Ion Sponge―Like V-Based Polyoxometalate: Toward High-Performance Cathode for Rechargeable Sodium Ion Batteries. ACS Nano, 2017, 11, 6911-6920.	7.3	95
36	In vitro biodegradation of three brushite calcium phosphate cements by a macrophage cell-line. Biomaterials, 2006, 27, 4557-4565.	5.7	94

#	Article	IF	CITATIONS
37	Chemical Reaction Between Ag Nanoparticles and TCNQ Microparticles in Aqueous Solution. Small, 2011, 7, 1242-1246.	5.2	92
38	Semi-Supervised Dimension Reduction Using Trace Ratio Criterion. IEEE Transactions on Neural Networks and Learning Systems, 2012, 23, 519-526.	7.2	91
39	Confining Tiny MoO ₂ Clusters into Reduced Graphene Oxide for Highly Efficient Low Frequency Microwave Absorption. Small, 2020, 16, e2001686.	5.2	87
40	Photochemically Controlled Synthesis of Anisotropic Au Nanostructures: Platelet-like Au Nanorods and Six-Star Au Nanoparticles. ACS Nano, 2010, 4, 6196-6202.	7.3	82
41	Characterisation of titanium oxide film grown in 0.9% NaCl at different sweep rates. Electrochimica Acta, 2005, 51, 1099-1107.	2.6	78
42	Growth of Tapered SiC Nanowires on Flexible Carbon Fabric: Toward Field Emission Applications. Journal of Physical Chemistry C, 2012, 116, 12940-12945.	1.5	78
43	Hierarchically porous three-dimensional electrodes of CoMoO ₄ and ZnCo ₂ O ₄ and their high anode performance for lithium ion batteries. Nanoscale, 2014, 6, 10556.	2.8	77
44	Multi-channel FeP@C octahedra anchored on reduced graphene oxide nanosheet with efficient performance for lithium-ion batteries. Carbon, 2018, 139, 477-485.	5.4	75
45	One-pot sequential electrochemical deposition of multilayer poly(3,4-ethylenedioxythiophene):poly(4-styrenesulfonic acid)/tungsten trioxide hybrid films and their enhanced electrochromic properties. Journal of Materials Chemistry A, 2014, 2, 2708-2717.	5.2	74
46	High-Crystallinity Urchin-like VS ₄ Anode for High-Performance Lithium-Ion Storage. ACS Applied Materials & Interfaces, 2018, 10, 14727-14734.	4.0	74
47	Hybrid vertical graphene/lithium titanate–CNTs arrays for lithium ion storage with extraordinary performance. Journal of Materials Chemistry A, 2017, 5, 8916-8921.	5.2	71
48	Enabling a Stable Room-Temperature Sodium–Sulfur Battery Cathode by Building Heterostructures in Multichannel Carbon Fibers. ACS Nano, 2021, 15, 5639-5648.	7.3	70
49	New insight into the roles of oxygen vacancies in hematite for solar water splitting. Physical Chemistry Chemical Physics, 2017, 19, 1074-1082.	1.3	69
50	A Bulk-Heterostructure Nanocomposite Electrolyte of Ce0.8Sm0.2O2-δ–SrTiO3 for Low-Temperature Solid Oxide Fuel Cells. Nano-Micro Letters, 2021, 13, 46.	14.4	66
51	Self-assembled Cu-Ni bimetal oxide 3D in-plane epitaxial structures for highly efficient oxygen evolution reaction. Applied Catalysis B: Environmental, 2019, 244, 56-62.	10.8	62
52	Hierarchical three-dimensional Fe3O4@porous carbon matrix/graphene anodes for high performance lithium ion batteries. Electrochimica Acta, 2018, 260, 965-973.	2.6	61
53	A novel synthesis of carbon nanotubes directly from an indecomposable solid carbon source for electrochemical applications. Journal of Materials Chemistry A, 2016, 4, 2137-2146.	5.2	59
54	Rational design of intertwined carbon nanotubes threaded porous CoP@carbon nanocubes as anode with superior lithium storage. Carbon, 2019, 142, 269-277.	5.4	58

#	Article	IF	CITATIONS
55	Nanoscale ion intermixing induced activation of Fe ₂ O ₃ /MnO ₂ composites for application in lithium ion batteries. Journal of Materials Chemistry A, 2017, 5, 8510-8518.	5.2	57
56	Nanostructured Metal–Organic Conjugated Coordination Polymers with Ligand Tailoring for Superior Rechargeable Energy Storage. Small, 2019, 15, e1903188.	5.2	57
57	Sb-Induced Phase Control of InAsSb Nanowires Grown by Molecular Beam Epitaxy. Nano Letters, 2015, 15, 1109-1116.	4.5	55
58	Phase transition of hollow-porous α-Fe ₂ O ₃ microsphere based anodes for lithium ion batteries during high rate cycling. Journal of Materials Chemistry A, 2016, 4, 16569-16575.	5.2	54
59	Preparation of Electrochemical Sensor Based on Zinc Oxide Nanoparticles for Simultaneous Determination of AA, DA, and UA. Frontiers in Chemistry, 2020, 8, 592538.	1.8	54
60	Characterization of corrosion products formed on the surface of carbon steel by Raman spectroscopy. Journal of Raman Spectroscopy, 2009, 40, 76-79.	1.2	53
61	Dependence of the corrosion behavior of aluminum alloy 7075 on the thin electrolyte layers. Materials Science and Engineering B: Solid-State Materials for Advanced Technology, 2009, 162, 1-8.	1.7	53
62	A general approach towards multi-faceted hollow oxide composites using zeolitic imidazolate frameworks. Nanoscale, 2015, 7, 965-974.	2.8	53
63	High thermoelectric performance enabled by convergence of nested conduction bands in Pb7Bi4Se13 with low thermal conductivity. Nature Communications, 2021, 12, 4793.	5.8	53
64	Cadmium Sulfide Quantum Dots Supported on Gallium and Indium Oxide for Visible‣ightâ€Driven Hydrogen Evolution from Water. ChemSusChem, 2014, 7, 2537-2544.	3.6	52
65	Templated formation of porous Mn 2 O 3 octahedra from Mn-MIL-100 for lithium-ion battery anode materials. Materials and Design, 2016, 98, 319-323.	3.3	52
66	Graphene reinforced nickel-based superalloy composites fabricated by additive manufacturing. Materials Science & Engineering A: Structural Materials: Properties, Microstructure and Processing, 2020, 769, 138484.	2.6	52
67	A Depth-Profiling Study on the Solid Electrolyte Interface: Bis(fluorosulfuryl)imide Anion toward Improved K ⁺ Storage. ACS Applied Energy Materials, 2019, 2, 7942-7951.	2.5	51
68	Cathodic plasma driven self-assembly of HEAs dendrites by pure single FCC FeCoNiMnCu nanoparticles as high efficient electrocatalysts for OER. Chemical Engineering Journal, 2021, 425, 131533.	6.6	51
69	Diffusion induced concave Co3O4@CoFe2O4 hollow heterostructures for high performance lithium ion battery anode. Energy Storage Materials, 2016, 4, 145-153.	9.5	50
70	Carbon supported Pt9Sn1 nanoparticles as an efficient nanocatalyst for glycerol oxidation. Applied Catalysis B: Environmental, 2016, 180, 78-85.	10.8	50
71	Engineering of cation and anion vacancies in Co3O4 thin nanosheets by laser irradiation for more advancement of oxygen evolution reaction. Nano Energy, 2021, 83, 105800.	8.2	50
72	Computational simulation of metastable pitting of stainless steel. Electrochimica Acta, 2009, 54, 6389-6395.	2.6	49

#	Article	IF	CITATIONS
73	Nanostructured CuO/C Hollow Shell@3D Copper Dendrites as a Highly Efficient Electrocatalyst for Oxygen Evolution Reaction. ACS Applied Materials & amp; Interfaces, 2018, 10, 23807-23812.	4.0	49
74	Hierarchical layered titanate microspherulite: formation by electrochemical spark discharge spallation and application in aqueous pollutant treatment. Journal of Materials Chemistry, 2010, 20, 10169.	6.7	48
75	Formation of VO2 zero-dimensional/nanoporous layers with large supercooling effects and enhanced thermochromic properties. RSC Advances, 2013, 3, 7124.	1.7	47
76	Highly Stable and Ultrahighâ€Rate Li Metal Anode Enabled by Fluorinated Carbon Fibers. Small, 2021, 17, e2006002.	5.2	47
77	Morphology controlled lithium storage in Li ₃ VO ₄ anodes. Journal of Materials Chemistry A, 2018, 6, 456-463.	5.2	46
78	Well-aligned SiC nanoneedle arrays for excellent field emitters. Materials Letters, 2013, 91, 220-223.	1.3	44
79	Interface reaction between an electroless Ni–Co–P metallization and Sn–3.5Ag lead-free solder with improved joint reliability. Acta Materialia, 2014, 71, 69-79.	3.8	44
80	Mechanistic Aspect of Non-Steady Electrochemical Characteristic During Stress Corrosion Cracking of an X70 Pipeline Steel in Simulated Underground Water. Corrosion, 2014, 70, 678-685.	0.5	43
81	The roles of lithium-philic giant nitrogen-doped graphene in protecting micron-sized silicon anode from fading. Scientific Reports, 2015, 5, 15665.	1.6	42
82	TEM investigation of intergranular stress corrosion cracking for 316 stainless steel in PWR environment. Acta Materialia, 2006, 54, 635-641.	3.8	41
83	Synthesis of Nanosize Powders and Thin Films of Yb-Doped YAG by Solâ^'Gel Methods. Chemistry of Materials, 2003, 15, 3474-3480.	3.2	40
84	Investigation of work softening mechanisms and texture in a hot deformed 6061 aluminum alloy at high temperature. Materials Science & Engineering A: Structural Materials: Properties, Microstructure and Processing, 2014, 606, 240-247.	2.6	40
85	The Self-Passivation Mechanism in Degradation of BiVO4 Photoanode. IScience, 2019, 19, 976-985.	1.9	40
86	Conductivity Modulation of 3Dâ€Printed Shellular Electrodes through Embedding Nanocrystalline Intermetallics into Amorphous Matrix for Ultrahigh urrent Oxygen Evolution. Advanced Energy Materials, 2021, 11, 2100968.	10.2	40
87	Porous and hollow NiO microspheres for high capacity and long-life anode materials of Li-ion batteries. Materials and Design, 2016, 92, 160-165.	3.3	39
88	High Thermoelectric Performance through Crystal Symmetry Enhancement in Triply Doped Diamondoid Compound Cu ₂ SnSe ₃ . Advanced Energy Materials, 2021, 11, 2100661.	10.2	39
89	Influence of pulsed laser deposition rate on the microstructure and thermoelectric properties of Ca3Co4O9 thin films. Journal of Crystal Growth, 2009, 311, 4123-4128.	0.7	38
90	Improving Photocatalytic H ₂ Evolution of TiO ₂ via Formation of {001}–{010} Quasi-Heterojunctions. Journal of Physical Chemistry C, 2013, 117, 22894-22902.	1.5	38

#	Article	IF	CITATIONS
91	Copper phosphide decorated g-C3N4 catalysts for highly efficient photocatalytic H2 evolution. Journal of Colloid and Interface Science, 2022, 610, 126-135.	5.0	37
92	Synthesis of metal sulfide sensitized zinc oxide-based core/shell/shell nanorods and their photoelectrochemical properties. Journal of Power Sources, 2014, 268, 388-396.	4.0	36
93	Phase controllable fabrication of zinc cobalt sulfide hollow polyhedra as high-performance electrocatalysts for the hydrogen evolution reaction. Nanoscale, 2018, 10, 1774-1778.	2.8	36
94	Enhancing the Electrochemical Performance of LiNi _{0.4} Co _{0.2} Mn _{0.4} O ₂ by V ₂ O ₅ /LiV ₃ O ₈ Coating. ACS Applied Materials & Interfaces, 2019, 11, 26994-27003.	4.0	36
95	Nitrogen configuration dependent holey active sites toward enhanced K+ storage in graphite foam. Journal of Power Sources, 2019, 419, 82-90.	4.0	36
96	High Performance Li Metal Anode Enabled by Robust Covalent Triazine Frameworkâ€Based Protective Layer. Advanced Functional Materials, 2021, 31, 2006159.	7.8	36
97	Effects of temperature on the chemistry and tribology of co-sputtered MoSx-Ti composite thin films. Thin Solid Films, 2005, 489, 137-144.	0.8	35
98	Phase Transformation of GeO ₂ Glass to Nanocrystals under Ambient Conditions. Nano Letters, 2018, 18, 3290-3296.	4.5	35
99	Superior Li-ion storage of VS ₄ nanowires anchored on reduced graphene. Nanoscale, 2019, 11, 9556-9562.	2.8	35
100	Effect of applied potentials on stress corrosion cracking of X70 pipeline steel in alkali solution. Materials & Design, 2009, 30, 2259-2263.	5.1	34
101	Preparation of site specific transmission electron microscopy plan-view specimens using a focused ion beam system. Journal of Vacuum Science & Technology an Official Journal of the American Vacuum Society B, Microelectronics Processing and Phenomena, 2001, 19, 755.	1.6	33
102	Solution-processable semiconducting thin-film transistors using single-walled carbon nanotubes chemically modified by organic radical initiators. Chemical Communications, 2009, , 7182.	2.2	33
103	Synthesis of Porous Amorphous FePO ₄ Nanotubes and Their Lithium Storage Properties. Chemistry - A European Journal, 2013, 19, 1568-1572.	1.7	33
104	Study on the correlation between passive film and AC corrosion behavior of 2507 super duplex stainless steel in simulated marine environment. Journal of Electroanalytical Chemistry, 2020, 864, 114072.	1.9	33
105	Atomically Dispersed Intrinsic Hollow Sites of <i>M</i> â€ <i>M</i> ₁ â€ <i>M</i> (<i>M</i> ₁ Â= Pt, Ir; <i>M</i> Â= Fe, Co, Ni, Cu, Pt, Ir) on FeCoNiCuPtlr Nanocrystals Enabling Rapid Water Redox. Advanced Functional Materials, 2022, 32, .	7.8	33
106	Polyphenylene Dendrimerâ€Templated In Situ Construction of Inorganic–Organic Hybrid Riceâ€Shaped Architectures. Advanced Functional Materials, 2010, 20, 43-49.	7.8	32
107	Direct evidence of passive film growth on 316 stainless steel in alkaline solution. Materials Characterization, 2017, 131, 168-174.	1.9	32
108	Probing the Performance Limitations in Thin-Film FeVO ₄ Photoanodes for Solar Water Splitting. Journal of Physical Chemistry C, 2018, 122, 9773-9782.	1.5	32

#	Article	IF	CITATIONS
109	The significance of carbon on the microstructure of TiAlNC coatings deposited by reactive magnetron sputtering. Applied Surface Science, 2006, 253, 2470-2473.	3.1	31
110	Dualâ€Phase Titanate/Anatase with Nitrogen Doping for Enhanced Degradation of Organic Dye under Visible Light. Chemistry - A European Journal, 2011, 17, 2575-2578.	1.7	31
111	Oneâ€Step Solvothermal Synthesis of Singleâ€Crystalline TiOF ₂ Nanotubes with High Lithiumâ€Ion Battery Performance. Chemistry - A European Journal, 2012, 18, 4026-4030.	1.7	31
112	Confinement of single polyoxometalate clusters in molecular-scale cages for improved flexible solid-state supercapacitors. Nanoscale, 2020, 12, 11887-11898.	2.8	31
113	Polysomatic apatites. Acta Crystallographica Section B: Structural Science, 2010, 66, 1-16.	1.8	30
114	Solution Growth of Ultralong Gold Nanohelices. ACS Nano, 2017, 11, 5538-5546.	7.3	30
115	Innovative development on a p-type delafossite CuCrO2 nanoparticles based triethylamine sensor. Sensors and Actuators B: Chemical, 2020, 324, 128743.	4.0	29
116	Preparation of transmission electron microscopy cross-section specimens of crack tips using focused ion beam milling. Journal of Microscopy, 2002, 207, 129-136.	0.8	28
117	Development of polyoxometalate-anchored 3D hybrid hydrogel for high-performance flexible pseudo-solid-state supercapacitor. Electrochimica Acta, 2020, 329, 135181.	2.6	28
118	Large Piezoelectricity and Ferroelectricity in Mnâ€Doped (Bi _{0.5} Na _{0.5})TiO ₃ â€BaTiO ₃ Thin Film Prepared by Pulsed Laser Deposition. Journal of the American Ceramic Society, 2016, 99, 2347-2353.	1.9	27
119	Hollow Mesoporous Co(PO ₃) ₂ @Carbon Polyhedra as High Performance Anode Materials for Lithium Ion Batteries. Journal of Physical Chemistry C, 2019, 123, 8599-8606.	1.5	27
120	Cobalt tungsten phosphide with tunable W-doping as highly efficient electrocatalysts for hydrogen evolution reaction. Nano Research, 2021, 14, 4073-4078.	5.8	27
121	Carbon spheres anchored Co3O4 nanoclusters as an efficient catalyst for dye degradation. Applied Catalysis A: General, 2016, 513, 106-115.	2.2	26
122	Improving solar water-splitting performance of LaTaON2 by bulk defect control and interface engineering. Applied Catalysis B: Environmental, 2018, 226, 111-116.	10.8	26
123	Macrophage-mediated biodegradation of poly(DL-lactide-co-glycolide)in vitro. Journal of Biomedical Materials Research - Part A, 2006, 79A, 582-590.	2.1	25
124	Facile "Needle‧cratching―Method for Fast Catalyst Patterns Used for Large‧cale Growth of Densely Aligned Singleâ€Walled Carbonâ€Nanotube Arrays. Small, 2009, 5, 2061-2065.	5.2	25
125	Controlled Synthesis of Doubleâ€Wall <i>aâ€</i> FePO ₄ Nanotubes and their LIB Cathode Properties. Small, 2013, 9, 1036-1041.	5.2	25
126	Direct evidence of initial pitting corrosion. Electrochemistry Communications, 2008, 10, 1000-1004.	2.3	24

#	Article	IF	CITATIONS
127	A novel core–shell nanocomposite electrolyte for low temperature fuel cells. Journal of Power Sources, 2012, 201, 164-168.	4.0	24
128	Pt nanodendrites anchored on bamboo-shaped carbon nanofiber arrays as highly efficient electrocatalyst for oxygen reduction reaction. International Journal of Hydrogen Energy, 2013, 38, 16677-16684.	3.8	24
129	Recent review on electron transport layers in perovskite solar cells. International Journal of Energy Research, 2022, 46, 21441-21451.	2.2	24
130	Synthesis and photosensitivity of azobenzene functionalized hydroxypropylcellulose. RSC Advances, 2013, 3, 15909.	1.7	23
131	Nano-scale oxidation of copper in aqueous solution. Electrochemistry Communications, 2013, 26, 21-24.	2.3	23
132	The role of tin oxide surface defects in determining nanonet FET response to humidity and photoexcitation. Journal of Materials Chemistry C, 2014, 2, 940-945.	2.7	23
133	Microwave Absorption: Confining Tiny MoO ₂ Clusters into Reduced Graphene Oxide for Highly Efficient Low Frequency Microwave Absorption (Small 30/2020). Small, 2020, 16, 2070168.	5.2	23
134	Dual-Nitrogen-Doped Carbon Decorated on Na ₃ V ₂ (PO ₄) ₃ to Stabilize the Intercalation of Three Sodium Ions. ACS Applied Energy Materials, 2020, 3, 6870-6879.	2.5	23
135	Synthesis of flower-like cobalt, nickel phosphates grown on the surface of porous high entropy alloy for efficient oxygen evolution. Journal of Alloys and Compounds, 2021, 885, 160995.	2.8	23
136	In Situ Modification of Three-Dimensional Polyphenylene Dendrimer-Templated CuO Rice-Shaped Architectures with Electron Beam Irradiation. Journal of Physical Chemistry C, 2010, 114, 13465-13470.	1.5	22
137	Loading MIL-53(Al) with Ag nanoparticles: Synthesis, structural stability and catalytic properties. International Journal of Hydrogen Energy, 2014, 39, 14496-14502.	3.8	22
138	Facile fabrication of free-standing Cu2O–Au nanocomposite on Cu foil for high performance glucose sensing. Journal of Alloys and Compounds, 2020, 848, 156532.	2.8	22
139	Lotus root-like porous carbon for potassium ion battery with high stability and rate performance. Journal of Power Sources, 2020, 466, 228303.	4.0	22
140	An investigation of the tensile and compressive properties of Al6061 and its nanocomposites in as-cast state and in extruded condition. Materials Science & Engineering A: Structural Materials: Properties, Microstructure and Processing, 2014, 607, 589-595.	2.6	21
141	Extraordinary catalysis induced by titanium foil cathode plasma for degradation of water pollutant. Chemosphere, 2019, 214, 341-348.	4.2	21
142	Enhanced Catalytic Activity Induced by the Nanostructuring Effect in Pd Decoration onto Doped Ceria Enabling an Origami Paper Analytical Device for High Performance of Amyloid-β Bioassay. ACS Applied Materials & Interfaces, 2021, 13, 33937-33947.	4.0	21
143	In Situ Formation of Decavanadate-Intercalated Layered Double Hydroxide Films on AA2024 and their Anti-Corrosive Properties when Combined with Hybrid Sol Gel Films. Materials, 2017, 10, 426.	1.3	20
144	Ordered distributed nickel sulfide nanoparticles across graphite nanosheets for efficient oxygen evolution reaction electrocatalyst. International Journal of Hydrogen Energy, 2019, 44, 1544-1554.	3.8	20

#	Article	IF	CITATIONS
145	Photoinduced superhydrophilicity of TiO ₂ thin film with hierarchical Cu doping. Science and Technology of Advanced Materials, 2012, 13, 025001.	2.8	19
146	Mechanically Durable Memristor Arrays Based on a Discrete Structure Design. Advanced Materials, 2022, 34, e2106212.	11.1	19
147	Failure modes after exhaustion of dislocation glide ability in thin crystals. Science in China Series D: Earth Sciences, 1999, 42, 1-9.	0.9	18
148	Effects of cathodic potential on the local electrochemical environment under a disbonded coating. Journal of Applied Electrochemistry, 2009, 39, 697-704.	1.5	17
149	An investigation into different nickel and nickel–phosphorus stacked thin coatings for the corrosion protection of electrical contacts. Surface and Coatings Technology, 2016, 300, 95-103.	2.2	17
150	Solvothermal synthesis of Li3VO4: Morphology control and electrochemical performance as anode for lithium-ion batteries. International Journal of Hydrogen Energy, 2017, 42, 22167-22174.	3.8	17
151	Molecular-scale cage-confinement pyrolysis route to size-controlled molybdenum carbide nanoparticles for electrochemical sensor. Biosensors and Bioelectronics, 2020, 165, 112373.	5.3	17
152	In situ optical spectroscopic understanding of electrochemical passivation mechanism on sol–gel processed WO3 photoanodes. Journal of Energy Chemistry, 2022, 71, 20-28.	7.1	17
153	Influence of the chemical composition of the plating solution on the ability of nickel coatings to protect Nd2Fe14B magnets against corrosion. Journal of Magnetism and Magnetic Materials, 2001, 223, 103-111.	1.0	16
154	Hierarchical architecture of self-assembled carbon nitride nanocrystals. Journal of Materials Chemistry, 2007, 17, 1255.	6.7	16
155	Rapid fabrication of nanoneedle arrays by ion sputtering. Nanotechnology, 2008, 19, 015303.	1.3	16
156	Fast and Simple Construction of Efficient Solarâ€Waterâ€Splitting Electrodes with Micrometerâ€Sized Lightâ€Absorbing Precursor Particles. Advanced Materials Technologies, 2016, 1, 1600119.	3.0	16
157	Electrochemical Signature of <i>Escherichia coli</i> on Nickel Micropillar Array Electrode for Early Biofilm Characterization. ChemElectroChem, 2019, 6, 4674-4680.	1.7	16
158	Phase-Sequenced Deposition of Calcium Titanate/Hydroxyapatite Films with Controllable Crystallographic Texture onto Ti6Al4V by Triethyl Phosphate-Regulated Hydrothermal Crystallization. Crystal Growth and Design, 2009, 9, 3412-3422.	1.4	15
159	Anisotropic surface strain in single crystalline cobalt nanowires and its impact on the diameter-dependent Young's modulus. Nanoscale, 2013, 5, 11643.	2.8	15
160	Passivation of Nickel Nanoneedles in Aqueous Solutions. Journal of Physical Chemistry C, 2014, 118, 9073-9077.	1.5	15
161	The Electrochemical Response of Single Crystalline Copper Nanowires to Atmospheric Air and Aqueous Solution. Small, 2017, 13, 1603411.	5.2	15
162	Chemical Vapor Deposition of Superconducting FeTe _{1–<i>x</i>} Se _{<i>x</i>} Nanosheets. Nano Letters, 2021, 21, 5338-5344.	4.5	15

#	Article	IF	CITATIONS
163	Nanostructures of defects in CdZnTe single crystals. Journal of Crystal Growth, 2008, 311, 85-89.	0.7	14
164	Effect of Dissolved Oxygen on Stress Corrosion Cracking of X70 Pipeline Steel in Near-Neutral pH Solution. Corrosion, 2010, 66, 015006-015006-6.	0.5	14
165	A ZnO nanowire resistive switch. Applied Physics Letters, 2013, 103, 123114.	1.5	14
166	Effect of annealing temperature on the crystallization and oxygen sensing property of strontium titanate ferrite sol–gel thin films. Sensors and Actuators B: Chemical, 2013, 187, 20-26.	4.0	14
167	Towards Perfectly Ordered Novel ZnO/Si Nanoâ€Heterojunction Arrays. Small, 2014, 10, 344-348.	5.2	14
168	Corrosion Behavior of Pipeline Steel with Different Microstructures Under AC Interference in Acid Soil Simulation Solution. Journal of Materials Engineering and Performance, 2019, 28, 1698-1706.	1.2	14
169	Ternary duplex FeCoNi alloy prepared by cathode plasma electrolytic deposition as a high-efficient electrocatalyst for oxygen evolution reaction. Journal of Alloys and Compounds, 2022, 891, 161934.	2.8	14
170	Electrochemical behaviors of hierarchical copper nano-dendrites in alkaline media. Nano Research, 2018, 11, 4225-4231.	5.8	13
171	Self-organization of nanoneedles in Feâ^GaAs (001) epitaxial thin film. Applied Physics Letters, 2006, 88, 103104.	1.5	12
172	Raman and IR spectroscopy study of corrosion products on the surface of the hotâ€dip galvanized steel with alkaline mud adhesion. Journal of Raman Spectroscopy, 2009, 40, 656-660.	1.2	12
173	Selfâ€Organization of a Hybrid Nanostructure consisting of a Nanoneedle and Nanodot. Small, 2012, 8, 2807-2811.	5.2	12
174	A hybrid nanostructure array for gas sensing with ultralow field ionization voltage. Nanotechnology, 2013, 24, 175301.	1.3	12
175	In-situ Corrosion Characterization of API X80 Steel and Its Corresponding HAZ Microstructures in an Acidic Environment. Journal of Iron and Steel Research International, 2015, 22, 135-144.	1.4	12
176	Transparent Ceramic Materials. Topics in Mining, Metallurgy and Materials Engineering, 2015, , 29-91.	1.4	12
177	Atmospheric corrosion resistance of electroplated Ni/Ni–P/Au electronic contacts. Microelectronics Reliability, 2016, 60, 84-92.	0.9	12
178	Improved Corrosion Resistance of Co,Al-Alloyed NdFeB Magnetic Nanostructures Processed by Microwave Synthesis Techniques. IEEE Transactions on Magnetics, 2018, 54, 1-5.	1.2	12
179	Sol-gel synthesis of highly reproducible WO3 photoanodes for solar water oxidation. Science China Materials, 2020, 63, 2261-2271.	3.5	12
180	Highly Strained Au Nanoparticles for Improved Electrocatalysis of Ethanol Oxidation Reaction. Journal of Physical Chemistry Letters, 2020, 11, 3005-3013.	2.1	12

#	Article	IF	CITATIONS
181	Enhancement of Conductivity in Ceria-Carbonate Nanocomposites for LTSOFCs. Journal of Nano Research, 2009, 6, 197-203.	0.8	11
182	Fabrication of hybrid CuO/Pt/Si nanoarray for non-enzymatic glucose sensing. Electrochemistry Communications, 2013, 33, 138-141.	2.3	11
183	Catalysis of Au nano-pyramids formed across the surfaces of ordered Au nano-ring arrays. Journal of Catalysis, 2019, 377, 389-399.	3.1	11
184	Ordered micropillar array gold electrode increases electrochemical signature of early biofilm attachment. Materials and Design, 2020, 185, 108256.	3.3	11
185	Ni-Fe-MoO42- LDHs/epoxy resin varnish: A composite coating on carbon steel for long-time and active corrosion protection. Progress in Organic Coatings, 2020, 140, 105514.	1.9	11
186	Tunable low-dimensional self-assembly of H-shaped bichromophoric perylenediimide Gemini in solution. Nanoscale, 2020, 12, 3058-3067.	2.8	11
187	Corrosion-enhanced dislocation emission and motion resulting in initiation of stress corrosion cracking. Science in China Series D: Earth Sciences, 1997, 40, 235-242.	0.9	10
188	Self-organized amorphous material in silicon (001) by focused ion beam (FIB) system. Applied Surface Science, 2005, 252, 1954-1958.	3.1	10
189	Single-Nanowire Fuse for Ionization Gas Detection. Sensors, 2019, 19, 4358.	2.1	10
190	Strained Ultralong Silver Nanowires for Enhanced Electrocatalytic Oxygen Reduction Reaction in Alkaline Medium. Journal of Physical Chemistry Letters, 2021, 12, 2029-2035.	2.1	10
191	<i>In situ</i> growth of WO ₃ /BiVO ₄ nanoflowers onto cellulose fibers to construct photoelectrochemical/colorimetric lab-on-paper devices for the ultrasensitive detection of AFP. Journal of Materials Chemistry B, 2022, , .	2.9	10
192	Initiation of Fissure from Hydrogen Blister in Rail Steel. Corrosion, 2000, 56, 1046-1049.	0.5	9
193	Cross-Sectional Observation of Yttrium and Nickel Oxide Doped Ceria Powder. Journal of Nanoscience and Nanotechnology, 2009, 9, 3898-3903.	0.9	9
194	Charge transport in hierarchical α-Fe2O3 nanostructures. Applied Physics Letters, 2011, 99, 132105.	1.5	9
195	Interface Reaction Between Electroless Ni–Sn–P Metallization and Lead-Free Sn–3.5Ag Solder with Suppressed Ni3P Formation. Journal of Electronic Materials, 2014, 43, 4103-4110.	1.0	9
196	Significant enhancement of UV emission in ZnO nanorods subject to Ga+ ion beam irradiation. Nano Research, 2015, 8, 1857-1864.	5.8	9
197	Polymerizable ionic liquid-derived carbon for oxygen reduction and evolution. Journal of Applied Electrochemistry, 2017, 47, 351-359.	1.5	9
198	Direct Evidence of the Dynamic Growth of Nanotwinned Copper Grain upon Electron Beam Irradiation. Crystal Growth and Design, 2020, 20, 6493-6501.	1.4	9

#	Article	IF	CITATIONS
199	Electrically Tunable Wafer-Sized Three-Dimensional Topological Insulator Thin Films Grown by Magnetron Sputtering*. Chinese Physics Letters, 2020, 37, 057301.	1.3	9
200	Growth of Lattice Coherent Co 9 S 8 /Co 3 O 4 Nanoâ€Heterostructure for Maximizing the Catalysis of Coâ€Based Composites. ChemCatChem, 2020, 12, 2431-2435.	1.8	9
201	Gas-solid interfacial charge transfer in volatile organic compound detection by CuCrO ₂ nanoparticles. Nanotechnology, 2021, 32, 315501.	1.3	9
202	Facile "Scratching―Method with Common Metal Objects To Generate Large-Scale Catalyst Patterns Used for Growth of Single-Walled Carbon Nanotubes. ACS Applied Materials & Interfaces, 2009, 1, 1873-1877.	4.0	8
203	Elimination of impurity phase formation in FePt magnetic thin films prepared by pulsed laser deposition. Applied Surface Science, 2014, 288, 381-391.	3.1	8
204	Evidence of a nanosized copper anodic reaction in an anaerobic sulfide aqueous solution. RSC Advances, 2016, 6, 19937-19943.	1.7	8
205	Improved magnetic properties of Co0.5La Fe2.5–O4/FeCo composite powders by magnetic exchange–coupling effect. Journal of Magnetism and Magnetic Materials, 2019, 491, 165596.	1.0	8
206	Janus-like particles prepared through partial UV irradiation at the water/oil interface and their encapsulation capabilities. Colloids and Surfaces A: Physicochemical and Engineering Aspects, 2020, 589, 124460.	2.3	8
207	Hydrogen-inducing nanovoids in thin crystals of 310 stainless steel. Journal of Materials Science, 1998, 33, 4813-4819.	1.7	7
208	Metal-sulfide-decorated ZnO/Si nano-heterostructure arrays with enhanced photoelectrochemical performance. Materials Research Bulletin, 2017, 96, 503-508.	2.7	7
209	Heterogeneous electron transporting layer for reproducible, efficient and stable planar perovskite solar cells. Journal of Power Sources, 2019, 437, 226907.	4.0	7
210	Decomposition behavior in the early-stage oxidation of Sm2Co17-type magnets. Scripta Materialia, 2021, 200, 113911.	2.6	7
211	Control of nanostructures induced by ion sputtering. Nanotechnology, 2007, 18, 025305.	1.3	6
212	Study of Nano-Ag Particles Doped TiO ₂ Prepared by Photocatalysis. Journal of Nanoscience and Nanotechnology, 2009, 9, 3904-3908.	0.9	6
213	Understanding the Southeast Asian haze. Environmental Research Letters, 2017, 12, 084018.	2.2	6
214	Atomic-scale oxidation of a Sm2Co17-type magnet. Acta Materialia, 2021, 220, 117343.	3.8	6
215	Metal-organic framework derived Co ₃ Se ₄ @Nitrogen-doped porous carbon as a high-performance anode material for lithium ion batteries. Nanotechnology, 2020, 31, 215602.	1.3	6
216	Microfabrication of ZnO on a PTFE Template Patterned by Using Synchrotron Radiation. Journal of the Korean Physical Society, 2008, 53, 2796-2799.	0.3	6

#	Article	IF	CITATIONS
217	The influence of dissolved oxygen in solution on the titanium oxide growth at different sweep rates. Electrochimica Acta, 2006, 51, 3521-3525.	2.6	5
218	Solution-processed CuZn1â^'xAlxS2: a new memory material with tuneable electrical bistability. Journal of Materials Chemistry, 2012, 22, 20149.	6.7	5
219	Staging: Unraveling the Potassium Storage Mechanism in Graphite Foam (Adv. Energy Mater. 22/2019). Advanced Energy Materials, 2019, 9, 1970081.	10.2	5
220	Enhanced field emission of CuO nanowires by aluminum coating for volatile organic compound detection. Sensors and Actuators B: Chemical, 2022, 353, 131181.	4.0	5
221	Strained carbon steel as a highly efficient catalyst for seawater electrolysis. , 0, , .		5
222	Symmetric organization of self-assembled carbon nitride. Nanotechnology, 2007, 18, 335605.	1.3	4
223	A simple solvothermal route to controlled diameter germanium nanowires. Journal of Materials Chemistry, 2008, 18, 2011.	6.7	4
224	Influence of Ga + ion irradiation on the magnetisation reversal process and magnetoresistance in CoFe/Cu/CoFe/IrMn spin valves. Chinese Physics B, 2010, 19, 037505.	0.7	4
225	Twinning enhanced electrical conductivity and surface activity of nanostructured CuCrO2 gas sensor. Sensors and Actuators B: Chemical, 2021, 338, 129845.	4.0	4
226	Stereotaxically Constructed Graphene Modification of CuO-Cu2O/TiO2 Microspheres for Boosted Lithium and Sodium Storage Performance. Journal of Electronic Materials, 2022, 51, 47-56.	1.0	4
227	Bioactive CaTiO3 film prepared on the biomedical porous Ti–15Mo alloy by one-step hydrothermal treatment. Journal of Materials Research and Technology, 2021, 14, 202-209.	2.6	4
228	Abnormal Deviation of Temperature–Resistivity Correlation for Nanostructured Delafossite CuCrO ₂ Due to Local Reconfiguration. Journal of Physical Chemistry C, 2020, 124, 28555-28561.	1.5	4
229	The Properties and Structure Relationship of Half Metallic Magnetic Materials on GaAs. IEEE Transactions on Magnetics, 2009, 45, 4360-4363.	1.2	3
230	Tailoring out-of-plane magnetic properties of pulsed laser deposited FePt thin films by changing laser energy fluence. Applied Surface Science, 2014, 315, 37-44.	3.1	3
231	Ceramic Powder Synthesis. Topics in Mining, Metallurgy and Materials Engineering, 2015, , 93-189.	1.4	3
232	Three dimension (3D) hierarchical electrode (Au/rGO/CoPt3) for electrooxidation of ethanol in fuel cells. International Journal of Hydrogen Energy, 2018, 43, 12596-12602.	3.8	3
233	Simultaneous enhancements of magnetization and remanence in sufficiently exchange-coupled Co0.8Al0.2Nd Fe2â^'O4/Co7Fe3(Co) composites. Journal of Magnetism and Magnetic Materials, 2020, 498, 166150.	1.0	3
234	Flexible Au micro-array electrode with atomic-scale Au thin film for enhanced ethanol oxidation reaction. Nano Research, 2021, 14, 311-319.	5.8	3

#	Article	IF	CITATIONS
235	Hydrogen-induced cracking by nanovoids in 310 stainless steel. Science in China Series D: Earth Sciences, 1998, 41, 372-382.	0.9	2
236	Influence of Ga ⁺ ion irradiation on thermal relaxation of exchange bias field in exchange-coupled CoFe/IrMn bilayers. Chinese Physics B, 2011, 20, 057503.	0.7	2
237	The role of metal layers in the formation of metal–silicon hybrid nanoneedle arrays. Nanoscale, 2014, 6, 3078-3082.	2.8	2
238	The disparity of corrosion resistance between Ni/Au and Ni–P/Au electrical contacts in mixed flowing and salt spray tests. Journal of Materials Science, 2017, 52, 9834-9849.	1.7	2
239	A Unique Ionization Gas Sensor With Extraordinary Susceptibility of Sub-1-Volt. IEEE Sensors Journal, 2020, 20, 3423-3428.	2.4	2
240	Interfacial 2-hydrozybenzophenone passivation for highly efficient and stable perovskite solar cells. Journal of Power Sources, 2020, 475, 228665.	4.0	2
241	Magnetic Patterning of Co/Pt Multilayers by Ga+ Ion Irradiation. Journal of Electronic Materials, 2009, 38, 468-474.	1.0	1
242	THERMAL STABILITY OF LOW DOSE Ga+ ION-IRRADIATED MAGNETIC TUNNEL JUNCTIONS. International Journal of Modern Physics B, 2010, 24, 6211-6218.	1.0	1
243	Sintering and Densification (I)—Conventional Sintering Technologies. Topics in Mining, Metallurgy and Materials Engineering, 2015, , 291-394.	1.4	1
244	Grain Growth and Microstructure Development. Topics in Mining, Metallurgy and Materials Engineering, 2015, , 519-579.	1.4	1
245	Powder Characterization and Compaction. Topics in Mining, Metallurgy and Materials Engineering, 2015, , 191-290.	1.4	1
246	In-situ Scanning Micro-Electrochemical Characterization of Corrosion Inhibitors on Copper. International Journal of Electrochemical Science, 2016, , 4110-4119.	0.5	1
247	Carbon Nanomaterials Based on Carbon Nanotubes (CNTs). Advanced Structured Materials, 2016, , 25-101.	0.3	1
248	Atmospheric microplasma based binary Pt ₃ Co nanoflowers synthesis. Journal Physics D: Applied Physics, 2020, 53, 225201.	1.3	1
249	Selected Peer-Reviewed Papers from 2nd International Conference on Surfaces, Coatings and Nanostructured Materials (NANOSMAT 2007). Journal of Nanoscience and Nanotechnology, 2009, 9, 3353-3354.	0.9	Ο
250	Other Applications. Topics in Mining, Metallurgy and Materials Engineering, 2015, , 675-734.	1.4	0
251	Sintering and Densification of Transparent Ceramics. Topics in Mining, Metallurgy and Materials Engineering, 2015, , 467-517.	1.4	Ο
252	Laser Applications. Topics in Mining, Metallurgy and Materials Engineering, 2015, , 581-674.	1.4	0

#	Article	IF	CITATIONS
253	Bimetallic Nanostructures Fabricated by Atmospheric Microplasma. , 2020, , .		0